RSC Advances

ROYAL SOCIETY OF CHEMISTRY

www.rsc.org/advances

RSC Advances

ARTICLE

Sol-gel Synthesis of Mesoporous Spherical Zirconia

Yulei Chang,[a] Chen Wang,[c] Tongxiang Liang,*[a] Chunsong Zhao,[b] Xi Luo,[b] Ting Guo,[a] Jianghong Gong,[b] Hui Wu*[b]

Mesoporous spherical zirconia (ZrO_2) with the surface area of 113 m^2/g and the average pore size of 5.0 nm is prepared by sol-gel method with $ZrOCl_2 \cdot 8H_2O$ precursors and Sodium Dodecyl Sulfonate (SDS) templates with subsequent annealing at 500 °C in air. After calcinating at 700 °C, tetragonal phase transfers to monoclinic zirconia and the surface area is reduced to 26 m^2/g. The mesoporous spherical structure, which is assembled by aggregation of ZrO_2 nanoparticles, is confirmed by the characterizations of low and wide-angle X-ray Diffraction, Transmission Electron Microscopy (TEM), Scanning Electron Microscope (SEM). The mesoporous ZrO_2 with the surface area of 113 m^2/g has a higher adsorption for Cs ion (357 mg/g). For the 700 °C calcinated ZrO_2, the absorption capacity at equilibrium is only 188 mg/g.

Introduction

Inorganic nanomaterials with mesoporous structure have received great attentions due to large surface areas, easy functionalization, possibilities for applications in catalysis[1,2] and other favourable characteristics. Mesoporous materials with controllable morphologies, pore sizes, and variable composition is highly desired for their advanced applications[3]. While silica of mesoporous structure[4,5] was successfully applied in many fields, synthesis of mesoporous materials of a board range of transition metal oxides have aroused scientists' interests for multiple applications[6,7], since transition metal oxides can be effectively applied as catalyst supports[8,9], chemical sensors[10,11], solid oxide fuel cells[12] and photocatalystic materials[13]. ZrO_2 has better ion transfer performance and the concentration of oxygen vacancy because it has both acid sites and basic sites on surface. ZrO_2 can acts as not only the carrier but the catalyst for some reactions. Introducing a mesoporous structure into the transition metal oxides is a promising route to upgrade the properties.

As nuclear energy is developed rapidly nowadays, radioactive waste has become a big problem. Many countries are devoted to researching into ADS (accelerator driven systems) reactor[14] which is designed to accomplish the high level radioactive waste (HLW) disposal. When choosing the matrix used in the ADS fuel to absorb radioactive waste, the thermal and mechanical properties, activation with neutrons, and chemical compatibility with neighboring materials, irradiation resistance should be considered[15]. ZrO_2, MgO, $MgAl_2O_4$ and $Y_3Al_5O_{12}$ are usually considered as inert matrix for inert matrix fuel (IMF), among which, ZrO_2 is a promising candidate because of its excellent mechanical properties, including high strength, high hardness and high fracture toughness. Currently ZrO_2–Minor Actinides (MA) fuel is manufactured by infiltration route, the first step is the production of ZrO_2 kernels using sol-gel method, and then the calcinated ZrO_2 kernels are immersed in actinide solution so that the infiltrated kernels are obtained[16]. This infiltration method does have two limitations, 1) the ratio of MA to the matrix is too low and cannot be chosen freely, i.e., the content of MA, that can be infiltrated, is determined by the porosity of the kernels. 2) The size and distribution of pores in the ZrO_2 after calcinated are heterogeneous, resulting in the maldistribution of MA. The uneven distribution of MA further degrades properties of fuels. Nevertheless the ZrO_2 with mesoporous structure have a promising to enhance volume and homogeneity of adsorption for MA.

There are different ways to compound mesoporous ZrO_2, broadly separated into hydrothermal synthesis[17,18], non-hydration method[19], sol-gel method[20,21] and soft or hard template method[22]. Hudson and Knowles et al.[23] use CTMAB (Hexadecyl trimethyl ammonium Bromide) as template and $ZrOCl_2$ as the source of zirconium to react in the alkaline aqueous solution and then the precursor was calcinated in hydrothermal synthesis reactor to compound mesoporous ZrO_2. Pacheco et al.[24] used dodecyl dihydrogen phosphate as template and Zirconium (IV) Ethoxide as the source of zirconium to prepare mesoporous ZrO_2 in acid isopropyl alcohol solution. Dong et al.[25] invented a hard template method to prepare mesoporous oxide and the process was described as followed. Firstly, uniform mesoporous silica spheres prepared by Unger's method[26] are used as the template for the formation of mesoporous carbon sphere by the nanocasting technology[27], and then mesoporous ZrO_2 are obtained by

[a] State Key Laboratory of New Ceramics and Fine Processing, Institute of Nuclear and New Energy Technology, Tsinghua University, Beijing, 100084, China.
[b] State Key Laboratory of New Ceramics and Fine Processing, School of Materials Science and Engineering, Tsinghua University, Beijing, 100084, China.
[c] Beijing Key Laboratory of Fine Ceramics, Institute of Nuclear and New Energy Technology, Tsinghua University, Beijing, 100084, China.
† email: huiwu@tsinghua.edu.cn, txliang@tsinghua.edu.cn

templating the specific precursor with carbon sphere whereafter. Lu et al.[28] use sol-gel method to synthesis yttria-stabilized mesoporous ZrO_2. However, a facile technique that is easy to practice and inexpensive to synthesis uniform and high surface area sphere-shaped ZrO_2 with inner mesoporous structure is still lacking. In this work, we present a simple and practicable facile sol-gel approach with the aid of structure-directing surfactant to synthesize ZrO_2 nanoparticles with mesoporous structure. We use low-cost material $ZrOCl_2$ (zirconium oxychloride) and $CO(NH_2)_2$ (carbamide) as raw materials to prepare mesoporous zirconia by sol-gel method[29] with the aid of SDS (sodium dodecyl sulfate)[30] as template. Moreover, a novel and interesting structure is found in the ZrO_2 powders. An amount of zirconia spheres are obtained and mesopore spreading on sphere. The specific surface area of mesoporous ZrO_2 is quite high comparing with samples of the precious methods and becomes higher after aging in ammonia solution.

Experimental

Chemicals

$ZrOCl_2$ (≥99.0%), SDS (Sodium Dodecyl Sulfonate), $CO(NH_2)_2$ (≥99.0%) (Carbamide) and Ammonia solution (25%-28%) are purchased from Sinopharm Chemical reagent Co. Ltd. All chemicals are used as received without further purification.

Preparation

The following synthesis procedure is employed for the preparation of mesoporous zirconia nanoparticles. 1) 3.759 g SDS is dissolved in 400ml deionized water. The SDS solution is then stirred on the magnetic stirring apparatus for about 3h until SDS is totally dissolved in H_2O as solution A. 2) 0.25mol (15.02 g) carbamide and 0.1mol (32.21 g) $ZrOCl_2$ are dissolved in 100ml deionized water as solution B. 3) We inject solution B into solution A using injection pump in a rate of 0.6 ml/min, meanwhile, the mixture solution is heated in water bath to 75 °C. After injecting all the solution B into A, solution C is obtained with 28.0 mmol/L SDS and 0.5 mol/L carbamide and 0.2mol/L $ZrOCl_2$. 4) The C solution is turned to be viscous sol after reacting for 12 h at 75 °C. Afterward, the viscous sol is dried for 24h at 80 °C in air atmosphere under atmospheric pressure to obtain a porous solid mass (xerogel). 5) The porous solid mass is calcinated under air at 500 °C and 700 °C for 5 h and naturally cooled under air condition to remove the SDS surfactant and then the desired mesoporous ZrO_2 particles are obtained.

Characterization

The X-ray diffraction (XRD) analyses are used to identify the crystalline phase of the sample, which are performed on a SmartLab diffractometer (Cu Kα radiation, λ=1.5406 A) with an operating voltage of 40 kv and a current of 40 mA. Morphological characterization is obtained by means of scanning electron microscope (SEM) using MERLIN VP Compact with an accelerating voltage of 1.0 kV. When conducting the SEM analyses, a small quantity of ZrO_2 powder was dispersed in ethyl alcohol under ultrasound so that the nanoparticle can be dispersed homogeneously. Transmission electron microscopy (TEM) is accomplished using Tecnai G2 TEM with the operating voltage of 200kV. Nitrogen adsorption/desorption isotherms are obtained using a BEL Japan Inc. Belsorp-HP surface area analyser at 77 K. The surface areas are calculated by the Brunauer-Emmett-Teller (BET) method and the pore size distributions are calculated by the Barrett-Joyner-Halenda (BJH) method from the adsorption/desorption isotherm. The samples are prepared by ultrasonic dispersing the material in methanol and then dripped one drop on a carbon coated copper grid when doing TEM.

Adsorption experiments

The cesium ion (Cs^+) adsorption on ZrO_2 is investigated. Cesium is supplied as cesium chloride from Sigma–Aldrich Company. Stock solutions of the test reagent are prepared by dissolving CsCl in distilled water, the initial concentration is 150 mg/L, and the initial pH is adjusted to the value of 7.0 using dilute solution of sodium hydroxide. 40mg of ZrO_2 adsorbent is added into the solution at 25 °C. Then, the suspension is stirred for 5 hours. After centrifugation, the residual quantity of Cs^+ is determined by ICP-AES. The absorption capacity q_e(mg/g) at equilibrium is calculated: $q_e = (C_0-C_e)V/W$, where C_0(mg/L) and C_e(mg/L) are the concentrations of Cs^+ at initial and equilibrium, respectively. V(L) and W(g) are the volume of solution and the mass of adsorbent, respectively.

Results and Discussion

X-ray diffraction

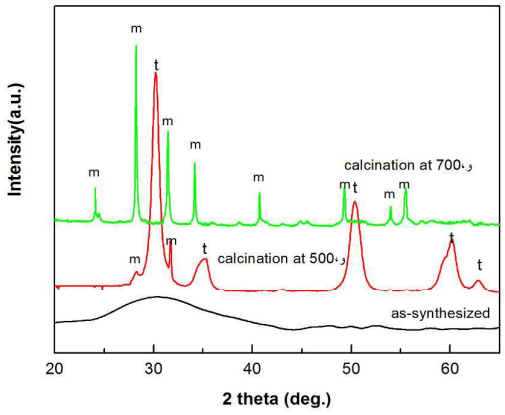

(a)

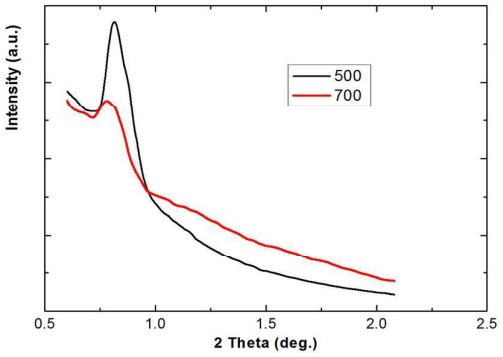

(b)

Fig. 1(a) XRD pattern of the synthesized mesoporous-assembled ZrO_2 nanoparticles; (b) XRD pattern in the low angle range of the synthesized mesoporous-assembled ZrO_2 nanoparticles.

As we can see in Fig. 1(a), the as-synthesized particles are amorphous. Two phase transformations are observed with increasing calcination temperature. The first one is a transformation from the amorphous state to crystalline tetragonal zirconia, which finished at about 500 °C. The second phase transformation is from tetragonal to monoclinic zirconia, which occurred after calcination at 700 °C. This transition from the amorphous to the metastable tetragonal phase and then to the thermodynamically stable monoclinic phase only after heating at higher temperatures is common and has been reported for zirconia particles[31,32]. For the first phase transformation, it is commonly accepted that the short-range order in the amorphous phase is more similar to the tetragonal rather than the monoclinic phase[32]. Thus, initial crystallization at 500 °C yields the metastable tetragonal phase, its XRD pattern correspond to the well crystallized with tetragonal phases (PDF number：89-6976), the primary crystal size is 6.4 nm as calculated by applying the Scherrer equation on the (011) diffraction peak. It has been reported that below a critical grain size, tetragonal rather than monoclinic becomes the thermodynamically preferred phase due to differences in the surface energies of the polymorphs. This critical size has been reported to be typically of the order of 10–20 nm[31].

Small-angle diffraction of ZrO_2 calcinated at 500 °C and 700 °C is done for the purpose of testing if there is mesoporous structure in this sample. The result is shown in Fig. 1(b). After calcinated at 500 °C, there is a peak and the beginning of the pattern which means there are mesopores in the material. But the peak intensity is reduced when the sample is calcinated at 700 °C, this means some mesopores disappeared.

Scanning electron microscope (SEM) and Transmission Electron Microscopy (TEM)

Fig. 2 shows that the obtained material is spherical particles with the size ranged from 100 nm to 300 nm. The inset of Fig.2 indicates that the surface of particles is not smooth and the spherical particles are agglomerates, i.e., they are composed of many tiny particles.

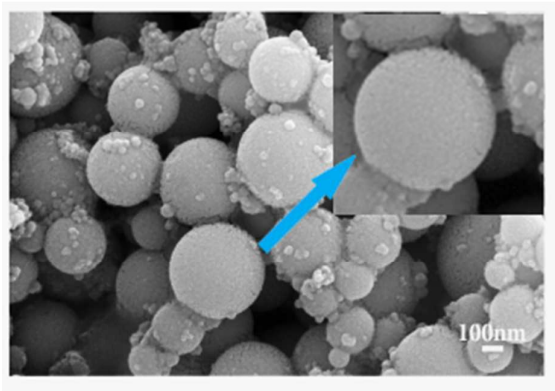

Fig. 2 SEM image of synthesized particles after calcinated at 500 °C, showing regular sphere morphologically.

The shape and size of ZrO_2 nanoparticles are controlled by synthesis method, stabilizer or surfactant[32], it is generally accepted that ZrO_2 particles are formed in two step mechanism[33]. First, ZrO_2 precursors are hydrolyzed and polymerized to form small primary particles in the size range of 1–10 nm, and then aggregate to form the final particles. As diffusion-limited aggregation mostly leads to disordered particles with no structural porosity, in Fig.2, one spherical particle is composed of many tiny particles, thus, the present reaction is believed to proceed via reaction-limited aggregation.

Fig.3 is the TEM and SAED images of ZrO_2 spherical particles after calcinated at 500 °C. As shown in Fig. 3(a) and (b), the particle is obviously spherical and many pores (about 5.0 nm in the length scale) spreading over the spheres, each sphere is composed of hundreds of individual tiny nanoparticles with an average diameter of about 5 nm, it can be conclude that the mesopore is created by assembly of zirconia nanoparticles. During calcination at 500 °C, amorphous zirconia transfers to tetragonal phase, rearrangement of the individual nanoparticles could occur, which results in the formation of strong covalent bridges between the particles. This covalent bonding between particles could be responsible for the high thermal stability of the mesoporous ZrO_2 nanoparticles. Thus, ZrO_2 nanocrystallites assembled to form thick mesoporous walls.

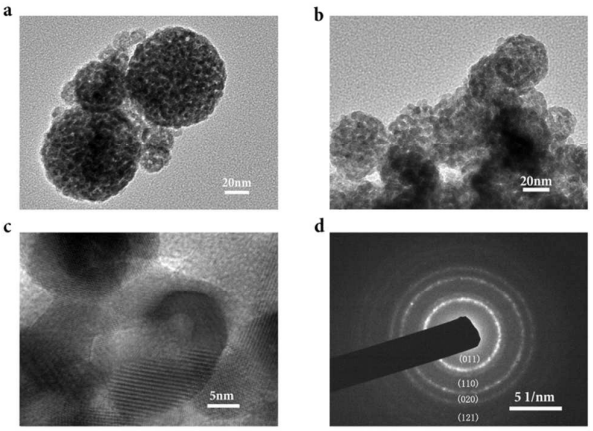

Fig. 3 (a) Low magnification TEM image of ZrO_2 sphere shows that big sphere is consist of tiny particle; (b) In the low magnification TEM image, the space between tiny particle is mesopore size; (c) High magnification TEM images of some particles; (d) SAED image of multicrystal ZrO_2.

Fig. 3(c) is the high magnification TEM image of some particles. As we can see in the picture, the pore wall is multicrystal and the lattice space of 0.3 nm assigned to the interplanar distance of the (101) planes of the sample. The corresponding Selected Area Electron Diffraction (SAED) pattern (Fig. 3(d)) of the spherical aggregates of ZrO_2 nanoparticles is indicative of high nanocrystallinity of the formed product and can be assigned to the tetragonal phase, the concentric Debye-Scherrer rings which can be indexed to the (011), (110), (020) and (121) planes. The *d*-spacing corresponding to the diffraction rings of the SAED pattern are in good agreement with the tetragonal phases of ZrO_2 nanocrystal.

Surface area and porosity

After calcinated at 500 °C, the spherical ZrO_2 nanoparticle scaffold exhibits a mesoporous channel system, displaying high surface areas and narrow pore size distribution. Fig. 4 shows N_2 adsorption-desorption isotherm of the sample calcinated at 500 °C, in which pore structure is confirmed clearly. The isotherm displays the typical type IV curve, which is usually attributed to the predominance of mesopores. The presence of a pronounced hysteresis loop in the isotherm curve is indicative for a 3D intersection network of the pores, which also goes well with the TEM observation. Moreover, the isotherms possess evident hysteresis loop with an evident increase in adsorbed N_2 volume in the relative pressure range of 0.45–0.90. This indicates the capillary condensation of N_2 molecules inside the sufficiently pores of small sizes. The average size of the mesopore is calculated to be about 5.0 nm.

The spherical ZrO_2 nanoparticle calcinated at 500 °C exhibits 113 m^2/g of surface area by a nitrogen Brunauer-Emmett-Teller (BET) measurement, which is rather high comparing with previous result. Qibing Chang[20] synthesized mesoporous ZrO_2 with the surface area of 43 m^2/g. After calcinated at 700 °C, the surface area of ZrO_2 nanoparticle reduced to 26 m^2/g. In bulk zirconia, phase transformation from tetragonal to monoclinic is accompanied by a volume expansion of 3–5%. This volume expansion will result in the collapse and disappear of mesopores.

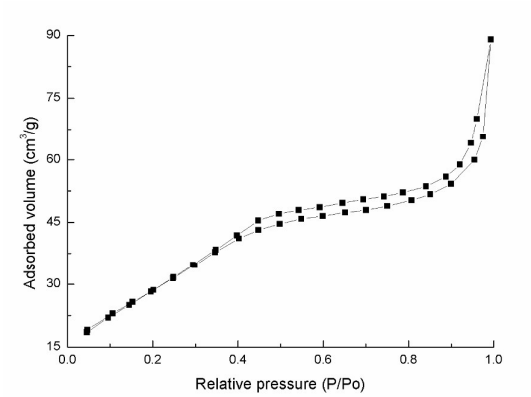

Fig. 4. N_2 adsorption-desorption isotherm of ZrO_2 calcinated at 500 °C

To explain the special morphology of mesoporous, in Fig.5, we suppose a model for the forming of mesoporous spherical ZrO_2 particles. When $ZrOCl_2 8H_2O$ is dissolved in water $[Zr_4(OH)_8(H_2O)_{16}]^{8+}$ complexation is formed, and carbamide is hydrolyzed to NH_4^+ and OH^-, then $Zr(OH)_{4-x}(OOH)_x$, is precipitated by the action of OH^-, finally ZrO_2 is produced during the subsequent heating. The whole reaction formula can be expressed as:

$4ZrOCl_2 8H_2O \rightarrow [Zr_4(OH)_8(H_2O)_{16}]^{8+} + 8Cl^- + 8H^+$ (1)

$CO(NH_2)_2 + 3H_2O \rightarrow 2NH_4^+ + 2OH^- + CO_2$ (2)

$[Zr_4(OH)_8(H_2O)_{16}]^{8+} + 8xOH^- \rightarrow 4Zr(OH)_{4-x}(OOH)_x^{-(2+2x)} + (24+8x)OH^-$ (3)

$Zr(OH)_{4-x}(OOH)_x \rightarrow ZrO_2$ (amorphous) $\rightarrow$ t-ZrO_2 or m-ZrO_2 (4)

$[Zr_4(OH)_8(H_2O)_{16}]^{8+}$ in aqueous solution generates $Zr(OH)_{4-x}(OOH)_x$ nanoparticles and grows slowly because of the slow introduction of OH^- from the release of carbamide, and these nanoparticles are adhere to the surface of SDS surfactant. During drying of the solvent, the surfactant induces cooperative assembly of functionalized nanoparticles to attain packing, results in the formation of large spherical particles. When the SDS template is removed from the particles, the mesopores are formed.

Fig.5. Mechanism for the forming of mesoporous spherical ZrO_2 particles

Adsorption of Cesium Ions on ZrO_2

It is known that pH is important factor for the adsorption of metal ions on adsorbents, because it affects the solution chemistry of the solute as well as the functional groups present in the sorbent. According to reference[34], zirconia contains hydroxyl groups which can act role in ion-exchange reaction through the substitution of its protons by cesium ion, the reactions is:

$nCs^+ + Zr(-OH)_m \leftrightarrow Zr(-O-Cs)_{m-n} + nH^+$ (1)

Where -OH is hydroxyl group, nH^+ is number of protons released, and Zr refers to the zirconia surface. The adsorption process is influenced by pH, contact time and temperature. The highest removal efficiency of zirconia for cesium ion was obtained at pH 7.0[35]. In this paper we fix the experimental parameters as: pH=7, Temperature=25°, the purpose is to compare the adsorption capacity of several kinds of powder on Cs ion. The adsorption equilibrium is reached within 2 hours. Table 1 shows the adsorption capacity of Cs ion on ZrO_2, where Z5 means ZrO_2 calcinated at 500 °C, Z7 means ZrO_2 calcinated at 700 °C, and R is the data from reference [35].

Sample	surface area (m^2/g)	q_e(mg/g)
Z5	113	357
Z7	26	188
R	-	130

Table 1. The adsorption capacity of Cs ion

Our result indicates that the mesoporous ZrO_2 has a higher adsorption for Cs ion. Future work includes: adding Y to stable ZrO_2 phase, improving the specific surface area,

studying the effect of monoclinic and tetragonal phase on the adsorption behaviour, surface modification to improve the adsorption or selective adsorption capacity, and the adsorption behaviour of other radionuclides, etc..

Conclusions

In this work, we produce mesoporous sphere of zirconia from a simple sol-gel processing. Carbamide will release OH- when heated to 70 ℃ in acid solution and OH^- is the essential group of ZrO_2 precursor. After calcinated at the temperature of 500 ℃ under air condition, the sample exhibit regular nanospheriacle which consists of tiny particles. The space between these tiny particles is mesopore size and the surface area is as higher as 113 m^2/g. The adsorption for Cs ion on this kind of mesoporous spherical ZrO_2 is 357 mg/g. When calcinating at 700 ℃, tetragonal phase transfers to monoclinic zirconia and the surface area is reduced to 26 m^2/g, the adsorption for Cs ion is only 188 mg/g.

Acknowledgements

This work is supported by the National Natural Science Foundation of China (Grand No. 21271114 and No. 91326203); Tsinghua University independent research and development fund (20111080982) and Program for Changjiang Scholars and Innovative Research Team in University (IRT13026).

Notes and references

1 M. Labaki, H. Laversin, E. A. Zhilinskaya, A. Aboukaïs, and D. Courcot, Electron paramagnetic resonance investigation of the nature of active species involved in carbon black oxidation on ZrO_2 and Cu/ZrO_2 catalysts, *Catal. Commun.,* **17**, 64-70 (2012).

2 J. S. Beck, C. T. Chu, I. D. Johnson, C. T. Kresge, M. E. Leonowicz, W. J. Roth, and Vartuli, Synthesis of mesoporous crystalline material; U.S. Patent 5108725. 28 Apr. 1992.

3 Y. Y. Lyu, S. H. Yi, J. K. Shon, et al., Highly stable mesoporous metal oxides using nano-propping hybrid gemini surfactants, *J. Am. Chem. Soc.*, **126** [8] 2310-2311 (2004).

4 S. Sadasivan, and G. B. Sukhorukov. Fabrication of hollow multifunctional spheres containing MCM-41 nanoparticles and magnetite nanoparticles using layer-by-layer method, *J. Colloid. Interf. Sci.*, **304** [2] 437-441 (2006).

5 S. B. Yoon, J. Y. Kim, J. H. Kim, S. G. Park, C. W. Lee, and J. S. Yu, Template synthesis of nanostructured silica with hollow core and mesoporous shell structures, *Curr. Appl. Phys.*, **6** [6] 1059-1063 (2006).

6 H. Wang, Z. Wu, and Y. Liu, A simple two-step template approach for preparing carbon-doped mesoporous TiO2 hollow microsphere, *J. Phys. Chem. C.*, **113** [30] 13317-13324 (2009).

7 Z. Gan, and J Guan, Chemical self-assembly route to fabricate hollow barium ferrite submicrospheres, *Acta. Phys-Chim. Sin.*, **22** [2] 189 (2006).

8 M. Labaki, H. Laversin, E.A. Zhilinskaya, A. Aboukaïs, and D. Courcot, Electron Paramagnetic Resonance investigation of the nature of active species involved in carbon black oxidation on ZrO_2 and Cu/ZrO_2 catalysts, *Catal. Commun.*, **17**, 64–70 (2012).

9 X. Zhang, H. Su, and X. Yang, Catalytic performance of a three-dimensionally ordered macroporous Co/ZrO_2 catalyst in Fischer–Tropsch synthesis, *J. Mol. Catal. A: Chem.,* **360**, 16–25 (2012).

10 T. Liu, L. Li, and J. Yu, An electrochemical sulfur sensor based on ZrO_2 (MgO) as solid electrolyte and ZrS_2 + MgS as auxiliary electrode, *Sens. Actuators B: Chem.,* **139**, 501–504 (2009).

11 R. Zhang, X. Zhang, and S. Hu, High temperature and pressure chemical sensors based on Zr/ZrO_2 electrode prepared by nanostructured ZrO_2 film at Zr wire, *Sens. Actuators B: Chem.,* **149**, 143–154 (2010).

12 H. J. Cho, and G. M. Choi, Effect of milling methods on performance of Ni-Y_2O_3 stabilized ZrO_2 anode for solid oxide fuel cell, *J. Power Sources.,* **176**, 96–101 (2008).

13 A. A. Ashkarran, S. A. A. Afshar, S. M. Aghigh, and M. Kavianipour, Photocatalytic activity of ZrO_2 nanoparticles prepared by electrical arc discharge method in water, *Polyhedron,* **29**, 1370–1374 (2010).

14 F. Bianchi, C. Artioli, K. W. Burn, et al., Status and trend of core design activities for heavy metal cooled accelerator driven system, *Energ. Convers. Manage.,* **47** [17] 2698-2709 (2006).

15 C. D. Bowman, Accelerator-driven systems for nuclear waste transmutation, *Annu. Rev. Nucl. Part. S.*, **48** [1] 505-556 (1998).

16 J. Somers, A. Fernandez, Inert matrix kernels for actinide incineration in high temperature reactors, *Progress in Nuclear Energy,* **48**, 259–267 (2006).

17 J. L. Blin, R. Flamant, B. L. Su, Synthesis of nanostructured mesoporous zirconia using CTMABr–ZrOCl2·8H2O systems: a kinetic study of synthesis mechanism, *Int. J. Inorg. Mater.*, **3** [7] 959-972 (2001).

18 F. Schüth, U. Ciesla, S. Schacht, et al., Ordered mesoporous silicas and zirconias: Control on length scales between nanometer and micrometer, *Mater. Res. Bull.,* 34 [3] 483-494 (1999).

19 M. Inoue, H. Kominami, and T. Inui, Solvothermal synthesis of large surface area zirconia, *Res. Chem. Intermediat.,* 24 [5]

571-579 (1998).

20 Q.B.Chang, J.E.Zhou, Y.Q.Wang, G.Y.Meng, Preparation and characterization of unique zirconia crystals within pores via a sol-gel-hydrothermal method, *Adv. Powder Tech.*,4,20,371-374 (2009).

21 F. Heshmatpour, and R. A. Babadi, Synthesis and characterization of nanocrystalline zirconia powder by simple sol–gel method with glucose and fructose as organic additives, *Powder. Technol.,* 205 [1] 193-200 (2011).

22 A. G. Dong, et al., General synthesis of mesoporous spheres of metal oxides and phosphates. *J. Am. Chem. Soc.,* 125 [17] 4976-4977 (2003).

23 M. J. Hudson, and J. A. Knowles, Preparation and characterisation of mesoporous, high-surface-area zirconium (IV) oxide, *J. Mater. Chem.,* 6 [1] 89-95 (1996).

24 E. Zhao, O. Hernandez, G. Pacheco, et al., Thermal behavior and texture of mesoporous zirconia obtained from anionic surfactants, *J. Mater. Chem.,* 8 [7] 1635-1640 (1998).

25 A. Dong, N. Ren, Y. Tang, et al., General synthesis of mesoporous spheres of metal oxides and phosphates, *J. Am. Chem. Soc.,* 125 [17] 4976-4977 (2003).

26 M. Grün, G. Büchel, D. Kumar, et al., Rational design, tailored synthesis and characterisation of ordered mesoporous silicas in the micron and submicron size range, *Stud. Surf. Sci. Catal.,* 128, 155-165 (2000).

27 J. H. Smått, N. Schüwer, M. Järn, et al., Synthesis of micrometer sized mesoporous metal oxide spheres by nanocasting, *Micropor. Mesopor. Mat.,* 112 [1] 308-318 (2008).

28 B. Lu, and Y. S. Lin, Sol–gel synthesis and characterization of mesoporous yttria-stabilized zirconia membranes with graded pore structure, *J. Mater. Sci.,* 46 [21] 7056-7066 (2011).

29 F. Davar, A. Hassankhani, and M. R. Loghman-Estarki, Controllable synthesis of metastable tetragonal zirconia nanocrystals using citric acid assisted sol–gel method, *Ceram. Int.,* 39 [3] 2933-2941 (2013).

30 G. Duan, C. Zhang, A. Li, et al., Preparation and characterization of mesoporous zirconia made by using a poly (methyl methacrylate) template, *Nanoscale. Res. Lett.,* 3 [3] 118-122 (2008).

31 S. Shukla, S. Seal, Thermodynamic tetragonal phase stability in sol–gel derived nanodomains of pure zirconia, J. Phys. Chem. B., 108, 3395-3399 (2004).

32 J. Widoniak, S. Eiden-Assmann, G. Maret, Synthesis and characterisation of porous and non-porous monodisperse TiO2 and ZrO2 particles, Colloids Surfaces A Physicochem. Eng. Asp., 270, 329-334 (2005).

33 T. Ogihara, N. Mizutani, M. Kato, Processing of monodispersed ZrO2 powders, Ceram. Int. , 13, 35-40 (1987).

34 N.Khalid, S.Ahmad, A.Toheed, J. Ahmed. Potential of rice husks for antimony removal. Appl. Radiat. Isotopes., 52, 31-38 (2000).

35 S.M. Yakout, H. S. Hassan, Adsorption Characteristics of Sol Gel-Derived Zirconia for Cesium Ions from Aqueous Solutions, Molecules, 19, 9160-9172 (2014).

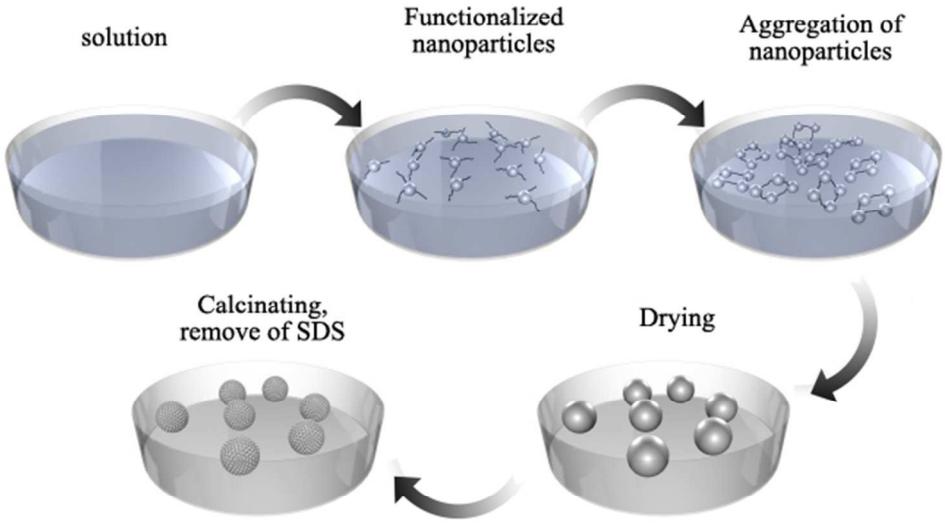

78x60mm (220 x 220 DPI)